



Preparation of carbon materials from chromium-tanned leather shavings for the removal of dyes from aqueous solution

Javier A. Arcibar-Orozco¹ · Bertha S. Barajas-Elías¹ · Hazael Baltazar-Campos¹ · Rene Rangel-Mendez²

Received: 5 April 2021 / Accepted: 6 July 2022 / Published online: 2 August 2022
© The Author(s) 2022

Abstract

Chromium-Tanned Leather Shavings are hazardous residues generated during leather processing. Since they contain considerable amounts of chromium, they represent a threat to life and the environment if managed improperly. The present study examines the transformation of such residues into carbon adsorbents and their use in the removal of azo dyes (methylene blue, Congo red and acid black 210) from water. The effects of temperature, holding time and the presence of an activating agent were studied, and basic characterization of the produced materials was performed. Carbon materials contain a low amount of chromium and an improved surface area that was only developed when high temperatures and an activating agent were employed. Depending on the synthesis conditions, the adsorbents' surface charge was positive or negative, which impacts the dye uptake from aqueous solution. Both the chemical speciation of the dye and the material's pore volume played a critical role during the adsorption process. It is possible to obtain carbon materials from Chromium-Tanned Leather Shavings, containing no hazardous chromium(VI) particles, that are capable of removing polluting dyes from water.

Keywords Chromium-tanned leather shavings · Carbon materials · Adsorption · Dye removal · Revalorization

Introduction

Every year tons of Chromium-tanned leather shavings (CTLS) residues are produced by the tanning industry (Pati et al. 2014). These residues are unavoidable and possess a considerable amount of Cr, and as such, they represent a major health and environmental hazard (Pati et al. 2014; Sundar et al. 2011). Unfortunately, they are normally discarded at the factory and dumped into landfills, where they can encounter oxidant conditions, releasing hazardous Cr(VI) into the air as particles and also into aqueous systems (Pati et al. 2014). In México, León city processes about 50,000 animal hides daily (González et al. 2017). That level of production, along with the recent development of

local, high-volume automotive manufacturing industry and its demand for large amounts of leather, has led to increases in the production of these shavings. This has exacerbated waste generation, further threatening the health and environment of León city.

In the search for sustainable development, not only must residue production be minimized, but viable technologies for waste recycling (downcycling) or valorization (upcycling) must also be developed. Among the several novel materials that can be obtained from the processing of these leather residues, their transformation into carbonaceous and activated carbon materials offers significant potential as a viable valorization technology (Kantarli and Yanik 2010; Louarrat et al. 2017; Oliveira et al. 2011; Arcibar-Orozco et al. 2019). During (activated) carbon production, the selection of the correct synthesis conditions led to the production of particular materials that are suited for specific environmental cleansing applications. When producing activated carbons from CTLS, temperature was found to be a critical limiting factor. The transition of chromium(III) to hazardous chromium(VI) occurred at processing temperatures higher than 600 °C (Erdem 2006), whereas temperatures that were too low resulted in incomplete pyrolysis and didn't promote correct pore development. Additionally, other parameters

✉ Javier A. Arcibar-Orozco
Javier.arcibar@gmail.com

¹ CIATEC A.C. Centro de Innovación Aplicada en Tecnología Competitiva, GTO, Omega 201, Industrial Delta, 37545 León, GTO, México

² División de Ciencias Ambientales, Instituto Potosino de Investigación Científica Y Tecnológica, A. C. Camino a la Presa San José 2055, Col. Lomas 4a Sección, 78216 San Luis Potosí, SLP, México

such as holding time and the concentration of the chemical activating agent could influence the development of pores and surface chemistry. ZnCl_2 was studied as a viable activating agent that allows for synthesis of activated carbon in one pyrolysis step at low temperatures (Marsh and Reinoso 2006: Activated Carbon). This agent has proven resistant to the decomposition and dehydration effects that it promotes in lignocellulosic precursor materials at medium–high temperatures (Nieto-Delgado et al. 2011). On other biomaterials like leather, which is mainly composed of collagen, the activation also occurs, but with different processing conditions and in a different way than in lignocellulosic materials.

Currently, the pollution of water bodies with dyes is of utmost importance as more than 700,000 tons of dyes are produced worldwide every year (Ahmad et al. 2015). About 90% of commercial dyes are of the azo type, and their removal from wastewater is desired for aesthetic reasons but also because they and/or their degradation products are toxic to aquatic life and some can even be carcinogenic (Tan et al. 2015). Adsorption is a cheap and feasible technology for dye pollution control; furthermore, when adsorbents are prepared from waste materials they can contribute to a closed loop of waste control.

In the present study, several carbon materials were prepared from CTLS using ZnCl_2 as an activant. The team studied synthesis conditions including temperature, holding time and ratio of ZnCl_2 . Synthesized materials were characterized and then employed for the removal of dye pollutants [acid black 210 (AB), methylene blue (MB) and Congo red (CR)] from aqueous solution. The focus of the present work is to contribute to the sustainable production of leather.

Materials and methods

Materials

All reagents used were analytical grade. The CTLS residues were provided from a local tannery located in León, Gto, Mexico; they resulted from the processing of cowhide. Deionized (DI) water with a conductivity of less than 0.217 $\mu\text{S}/\text{cm}$ was employed in all experiments.

Synthesis of carbonaceous materials

The CTLS collected were washed several times to remove debris, dust and other foreign compounds. They were then dried, crushed and sieved. A mesh with an opening between 1000 and 500 μm was selected as the particle size to be pyrolyzed. Next, a mass of about 20 g of CTLS was mixed with a selected mass of ZnCl_2 and then a volume of approximately 1 L of water was added. The mixture was kept under magnetic stirring for 24 h and then heated to 60 °C while

continuously stirring. Once most of the water evaporated, the mixture was transferred into a plastic container and heated in an oven to 80 °C where it was held for 24 h to evaporate the remaining water. After drying, a mass of about 2.0 g was measured into a boat crucible and placed in a tubular furnace. The furnace was flushed with nitrogen for at least 30 min before pyrolysis to remove any trace of oxygen in the system. An acidic water trap (pH 3) was placed at the end of the pyrolysis tube to collect soluble compounds from the fumes. After purging, the pyrolysis started at a heating rate of 10 °C/min up to the desired temperature for the appropriate holding time (Table 1). During pyrolysis, a 100 mL/min nitrogen flow was continuously feed into the system. After pyrolysis, the samples were washed with 0.1 M HCl until no traces of zinc were detected in the rinsing solution, then the samples were washed with DI water until the pH stabilized. Finally, the carbonaceous remains were dried at 90 °C for 24 h. Test nomenclature and synthesis conditions can be observed in Table 1.

Materials characterization

The inorganic content of the materials was evaluated by several techniques. The ash content was determined as the remaining weight of carbons after calcination at 600 °C for 2 h. Zinc and chromium content were determined by atomic absorption spectroscopy in iCE 3000 (Thermo), after acidic digestion with 20% HCl v/v. The experiments were carried out in triplicate and averages were plotted. The standard error was maintained within 1%. Organic content (C, H, N and S) was determined in an elemental analyzer Flash 2000 (Thermo). XRD analysis was obtained in a Bruker D8 Advance using a $\text{Cu}_{\text{K}\alpha}$ source. Fourier Transform Infrared Spectroscopy (FT-IR) was obtained in a Nicolet iS 10 (Thermo) operated in Attenuated Total Reflectance (ATR) mode. Microscopy observations were performed in a FEI HELIOS NANOLAB

Table 1 Nomenclature, synthesis conditions and yield of the materials prepared in this study

Name	ZnCl_2 /precursor mass ratio	Holding temperature (°C)	Holding time (h)	Yield (%)
C0_300_2	0	300	2	37.6
C0.5_300_2	0.5	300	2	48.3
C0_400_2	0	400	2	49.0
C0.5_400_1.5	0.5	400	1.5	39.0
C0.5_400_2	0.5	400	2	53.4
C1.0_400_1	1	400	1	50.7
C1.0_500_1.5	1	500	1.5	32.4
C1.0_600_2	1	600	2	35.0

600 Scanning Electron Microscope (SEM) with a secondary electron detector. Specific surface area was obtained from the corresponding nitrogen physisorption isotherm obtained in an ASAP 2020 (Micrometrics) by using the Brunauer-Emmett-Teller Method (BET). Surface charge distribution was obtained from the potentiometric titration of the materials performed in a 916 Ti-touch (Metrohm). Briefly, 100 mg of sample were contacted with 50 mL of a 0.1 M NaNO₃ electrolyte; the solution was continuously bubbled with nitrogen to avoid interference from CO₂ dissolution. The pH was decreased to 3 by adding 0.1 M HCl and then titrated with 0.1 M NaOH up to pH 11. The surface charge distribution was calculated using the formula:

$$Q = \frac{1}{m} [V_0 \{H_s - OH_s\} + V_t N_t - (V_0 + V_t) \{H_f - OH_f\}] \quad (1)$$

Here, Q is the amount of adsorbed or released protons from the surface (referred to as surface charge). V_0 and V_t are the solution and titrant added volumes. N_t is the normality of titrant, m is the titrated mass and the suffixes s and f stand for the starting and final concentrations of H⁺ and OH⁻ ions, determined by the Davies equation (Bandosz et al. 1993).

Adsorption experiments

The selected dyes were acid black 210 (AB), methylene blue (MB) and Congo red (CR); their chemical structures and sizes can be found in Fig. S1. A master solution of 1000 mg/L of each dye was prepared and from that, dilutions were made. A mass of 20 mg ± 1 mg of the carbon sample was placed in a 50-mL Falcon tube and then mixed with a 20 mL solution of the desired concentration of the selected dye. The experimental tubes were sealed and maintained at 25 °C for 5 days. All adsorption experiments were carried out at pH 7, and to ensure that this pH was maintained, it was adjusted daily by adding 0.1 M HCl and/or 0.1 M NaOH. Once equilibrium was reached, the solutions were filtered using inert filters (tests were performed to ensure filters did not affect the dye concentration) and analyzed in a UV-Vis spectrometer (Evolution 300, Thermo).

A mass balance was carried out in the adsorption reactor, and adsorption capacity was calculated by using the formula:

$$Q_{eq} = \frac{V(C_{eq} - C_0)}{m} \quad (2)$$

Here, Q_{eq} is the adsorption capacity, expressed as mass (or mole) of the dye per gram of adsorbent, reached at the equilibrium concentration C_{eq} in mg/L or μmol/L. C_0 is the starting dye concentration and m is the adsorbent mass in g.

Results and discussion

The yield of the pyrolysis, calculated as the mass that survived the pyrolysis divided by the precursor mass, is provided also in Table 1. As can be observed, yields were typically below a 50%, and in the best case 53.4% of mass remained after the pyrolysis process. As expected, the materials synthesized at the highest temperatures resulted in the largest burn-off, as a natural consequence of the conditions employed. Therefore, sample C0.5_400_2 had a high yield and low burn-off, since the low temperature did not allow for the material to be highly pyrolyzed. The characterization of the CTLS precursor material has been reported elsewhere (Arcibar-Orozco et al. 2019). The precursor material contains large amounts of nitrogen, that upon pyrolysis, can be incorporated in the matrix. This contributes to an increase in the yield; however this was not observed at high temperatures.

Ash content of the materials was relatively high (approximately about the same a mineral carbon), but below 15% in all materials (Fig. 1a). As the temperature and holding time increased, the ash content increased as well. This effect is related to the contribution of non-volatile inorganic mass, and the higher level of volatilization of organic carbon and nitrogen as temperature and time during pyrolysis increased. The inorganic mass made a marked contribution due to the chromium content resulting from the CTLS, and zinc leftovers from the chemical activating agent, see Fig. 1b. The chromium content is considerably higher than that of zinc because of its greater solubility; also chromium(III) is considerably less soluble than chromium(VI). During pyrolysis, the oxidation of chromium to a hexavalent state cannot be dismissed. Therefore, an acidic treatment was added during rinsing to ensure the removal of soluble hexavalent chromium from the carbon surface, hence only low soluble Cr(III) survived. Furthermore, chromium content was kept below 1% in all materials. At higher temperature tests, the team noted reduced chromium content within the carbon. This was a natural result of the volatilization of carbon, and likely, chromium as well. For that reason, an acidic solution was placed at the end of the production tube to collect all soluble fumes for chromium concentration analysis. The result demonstrated that only about 1% of precursor chromium is being volatilized and captured; therefore, most of the chromium from the precursor is being removed during acid treatment, and the rest is transformed into non-oxidized chromium particles. In a previous report of XPS measurements (Arcibar-Orozco et al. 2019), no presence of chromium(VI) particles was found in similar materials; even those in which acidic treatment was not applied.

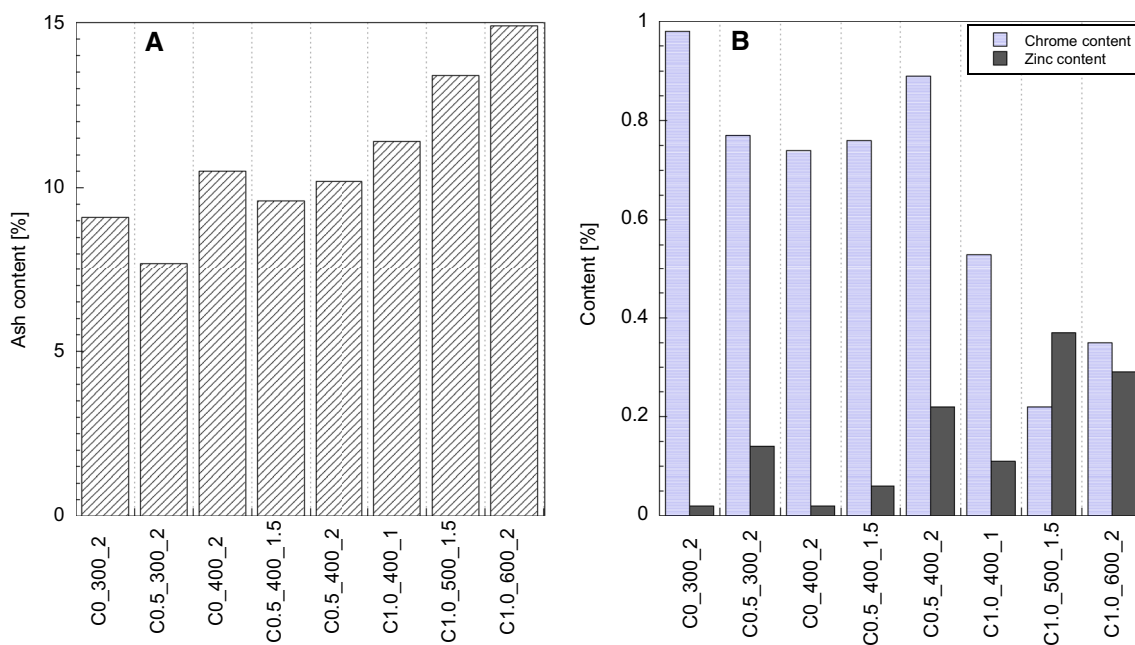


Fig. 1 a Ash content of the materials and b chromium and zinc contents

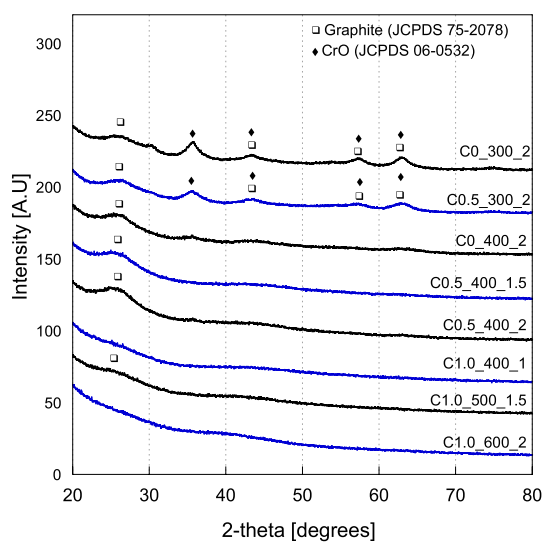


Fig. 2 X-Ray diffraction patterns of studied materials

The X-Ray measurements of the resulting carbons are provided in Fig. 2. As can be seen, most of the patterns do not display any particular crystallinity. The majority of the broadened peaks correspond to graphite, a normal pattern observed in carbons and activated carbons. Perhaps the most remarkable observations were found in the materials C0_300_2 and C0.5_300_2, which suggested the presence of CrO particles. These were only detected in samples prepared at low processing temperatures. Other than that, no

observations suggested the presence of crystalline forms of any chromium particle. This is probably due to the low amount of chromium present in the materials or that the resulting particles are too small to diffract.

For scanning electron microscopy, the materials C0.5_400_2 (Fig. 3b), and C1.0_500_1.5 (Fig. 3c–d) were selected. The surface of these materials was smooth and semi-flat, with homogeneous sphere-like macropores present. It is likely that these pores are vestiges of hair follicles removed during the preparation of skin for tanning. The particles observed in Fig. 3a and c are likely associated with Zn.

The results of FT-IR measurements are displayed in Fig. 4. The spectra of the materials depended on the carbonization temperature employed. The materials synthesized at 300 °C first displayed a wide peak corresponding to bulk hydroxyl groups at about 3200 cm^{-1} ; this band was also present in the material synthesized at 400 °C and 1 h. Since the materials prepared at higher temperatures do not display this wide peak, it is reasonable to attribute these vibrations to groups that decompose at higher temperatures. In these materials, a band with a shoulder at 2929 and 2863 cm^{-1} , respectively, was also observed. These can be attributed to C–CH₂ and C–CH₃ vibration bands resulting from the precursor material. As mentioned before, the decrease in these bands can be related to the decomposition of such groups at high temperatures. Bands at 1980 cm^{-1} can be related to C=O vibration of esters, which may come either from amino acid groups of proteins in the precursor materials, or from carboxylic groups formed in the surface of carbonized materials. Finally, bands at 1107 and 1032 cm^{-1} can be due

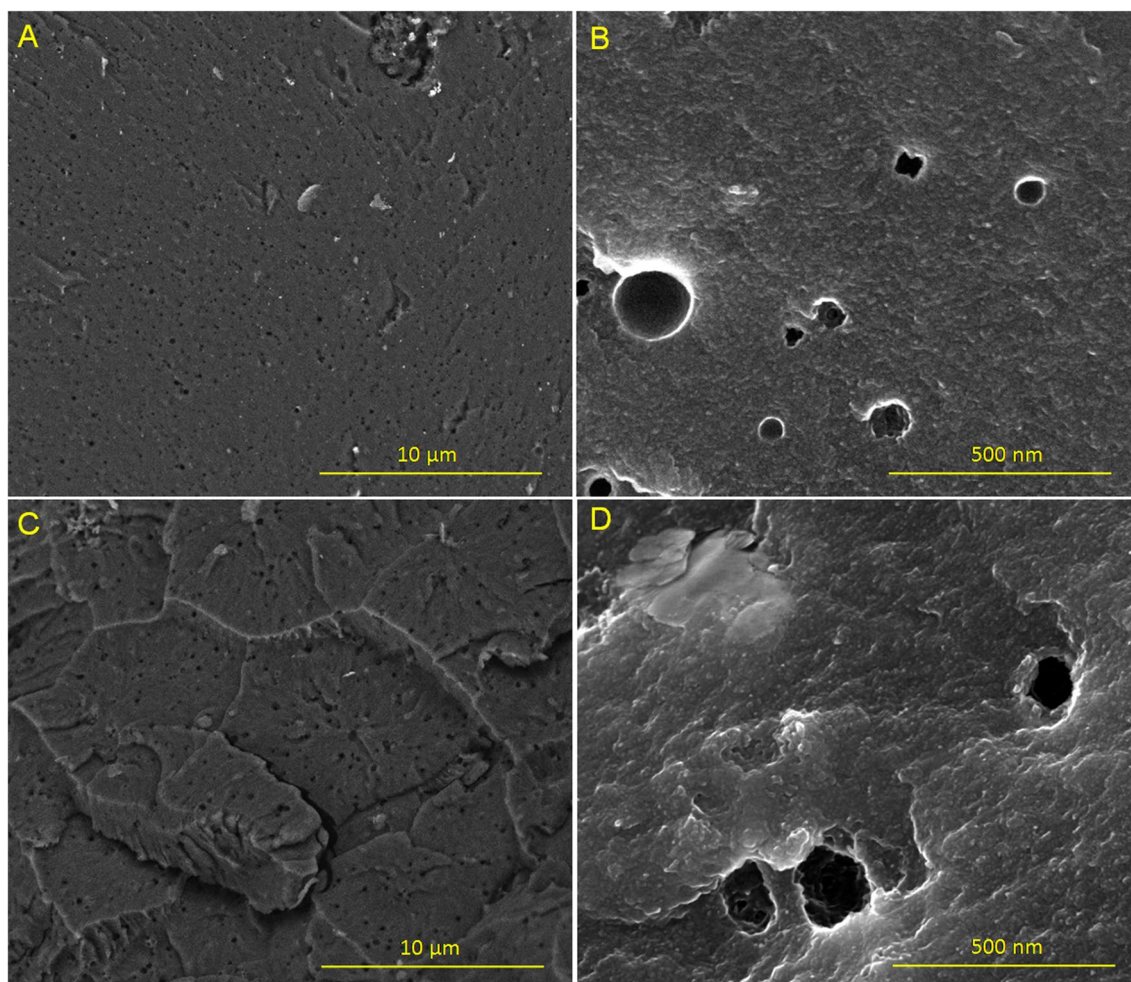


Fig. 3 SEM images of the surface of a–b C0.5_400_2; and c–d C1.0_500_1.5

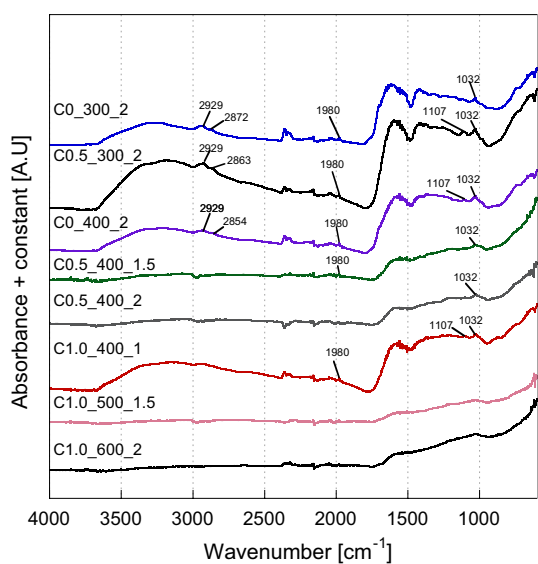


Fig. 4 FT-IR spectra of synthesized carbons

to C–O–C and C–O vibrations from carbon (Silverstein et al. 2005). Most of the information related to surface vibration of carbons was absent in the materials synthesized at high temperatures.

Surface chemical groups are very influential for the uptake of adsorbates from aqueous solution. The presence of dissociable groups on a material’s surface affects the development of charge. Therefore, the evaluation of the surface charge distribution (the capability of protons to bind to the surface) was important and determined by means of potentiometric titration experiments. The results are presented in Fig. 5. An experimental window of pH 4 to 10 was selected for displaying the results. There were significant differences noted across the tested materials. The intercept of the proton binding isotherm with the pH axis defines the point of zero net proton charge, or simply the point of zero charge (pH_{PZC}) (Sposito 1998). Based on the intercept value the materials were cataloged as acidic: C1.0_500_1.5 (pH_{PZC} ~ 4.15) followed by C1.0_600_2 (pH_{PZC} ~ 4.60), C0.5_300_2 (pH_{PZC} 4.91), C1.0_400_1 (pH_{PZC} ~ 5.27),

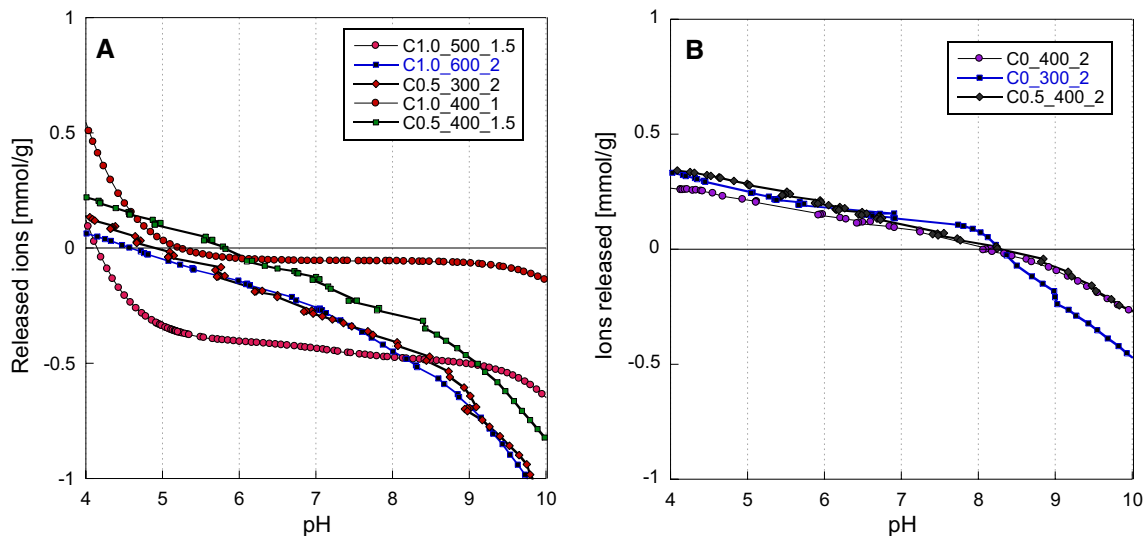


Fig. 5 Surface charge distribution of **a** acidic materials and **b** weak acidic materials

and C0.5_400_1.5 ($\text{pH}_{\text{PZC}} \sim 5.79$); to basic: C0_400_2 ($\text{pH}_{\text{PZC}} \sim 8.07$), C0_300_2 ($\text{pH}_{\text{PZC}} \sim 8.22$), and C0.5_400_2 ($\text{pH}_{\text{PZC}} \sim 8.25$). It is evident that higher pyrolysis temperatures resulted in the incorporation of acidic surface groups. Though it was not possible to determine the nature of such complex groups during FT-IR measurements, it is evident that their presence results in the release of protons from the surface. The shape of the proton-binding isotherm provides valuable information about the extent of surface groups. The C1.0_400_1 material was slightly acidic, and developed a subtle charge on the surface, whereas C1.0_500_1.5 developed a strong acidic charge that was strongly dissociated throughout almost the entire experimental window. Similarly, materials processed at low temperature were basic but with a slight positive charge, a result of the minimal amount of surface groups. The characterization results indicated that high temperatures (higher than 500 °C) are necessary to completely promote the carbonization of the precursor material, and only by using a high temperature (600 °C) was porosity developed. As the materials at different preparation conditions possess different surface charges, they will be expected to behave differently upon different colorants depending on the colorant's particular chemistry. As mentioned earlier the colorants selected include methylene blue, acid black 210 and Congo red. Not only they are useful model dyes, they also possess different chemical structures and molecular size, making them ideal for evaluating the role of chemical and structural features during adsorption. The surface area of the carbons is reported in Table 2. Each displayed very low surface areas with the exception of the material synthesized at 600 °C for 2 h, which had a surface area of 291 m²/g, this sample also had a considerable ash

Table 2 Surface area of the synthesized materials

Material	BET surface area (m ² /g)
C0_300_2	0.2
C0.5_300_2	0.9
C0_400_2	0.9
C0.5_400_1.5	0.8
C0.5_400_2	0.3
C1.0_400_1	0.6
C1.0_500_1.5	2
C1.0_600_2	291

content, which is a natural effect of the high burn-off that created a porous structure, therefore leaving an overall low carbon content.

Unlike what occurs in lignocellulosic materials, the pyrolysis of collagen-based precursors is not as well understood. The different fractions of the collagen have different decomposition temperatures. According to various authors, glycine decomposes at about 250 °C (Weiss et al. 2018), whereas proline decomposes at 220 °C (O'Neil 2013); hydroxyproline melting point has been reported at 275 °C (Olafsson and Bryan 1970). From C, H, S, and O analysis, it was determined that the carbon samples contain about 20% nitrogen (Table S1 Supplementary Information). Since degradation of such amino acids has been reported to produce only NH₃ as a nitrogen combustion product, it is reasonable to assume that nitrogen must be associated with oxygen rather than hydrogen on the surface of the carbons, therefore leading to the development of lactams, imides, and amine groups

Fig. 6 Results of the screening adsorption experiments, starting from a concentration of 100 ppm of the colorant, at pH 7, 25 °C and 120 h of contact. **a** Acid Black 210; **b** Methylene Blue; **c** Congo Red

on the carbons. These groups have a slightly acidic nature and are prone to acidification of the surface. It is clear that the various preparation conditions employed have different effects on the surface structure and chemistry, and in turn upon their capacity to remove the colorants studied.

Screening adsorption experiments were performed to evaluate the capability of the carbons to adsorb the colorants, and with those experiments, to select the best ones to build the isotherms. The results of these screenings are seen in Fig. 6 for A) methylene blue, B) acid black, and C) Congo red.

Several observations can be made from the adsorption results. In most cases the sample C1.0_500_1.5 was the best performing material for all colorants (for MB uptake, the capacity was almost the same as the C0_300_2 product). This material was also the one with the highest surface acidity of all, demonstrating the importance of negative charge development during adsorption. This suggests that electrostatic interactions are probably responsible for most of the uptake of the colorants. It is interesting to note that considering the speciation of the colorants, the predominant charge based on the dissociation/protonation of sites at pH 7 are positive for MB and for AB; however, CR is mainly dissociated [$pK_a=4.0$ (Elaziouti and Ahmed 2011)] and it is expected to undergo an electrostatic repulsion near the negatively charged surface of C1.0_500_1.5.

For these reasons, the C1_500_1.5 product was selected for obtaining adsorption isotherms at pH 7 and 25 °C. In order to compare them objectively, their adsorption capacities were given by molar unit. The results are shown in Fig. 7. Isotherms were correlated to the Langmuir and Freundlich adsorption isotherm models and the results are provided in Table 3. Both models correctly described the adsorption of the dyes, but the Freundlich model of adsorption was the more accurate. It is well known that a Freundlich isotherm model can be applied to multilayer adsorption over heterogeneous surfaces (Foo and Hameed 2010), such as presented in this study.

Due to the protonation of their thiazine ring and resulting positive charge development, adsorption of MB is favorable (Kannan and Sundaram 2001). Even though CR is dissociated at pH 7, it was still more readily adsorbed than AB. The reason is simple, CR could be adsorbed by means of $\pi-\pi$ interactions with the carbon's surface at both external surfaces and inside pores. The molecular size of the dyes is provided in Fig. S1. Here it is seen that dye molecular sizes are 1.26 nm for MB (Chen et al. 2015), 2.3 nm for CR

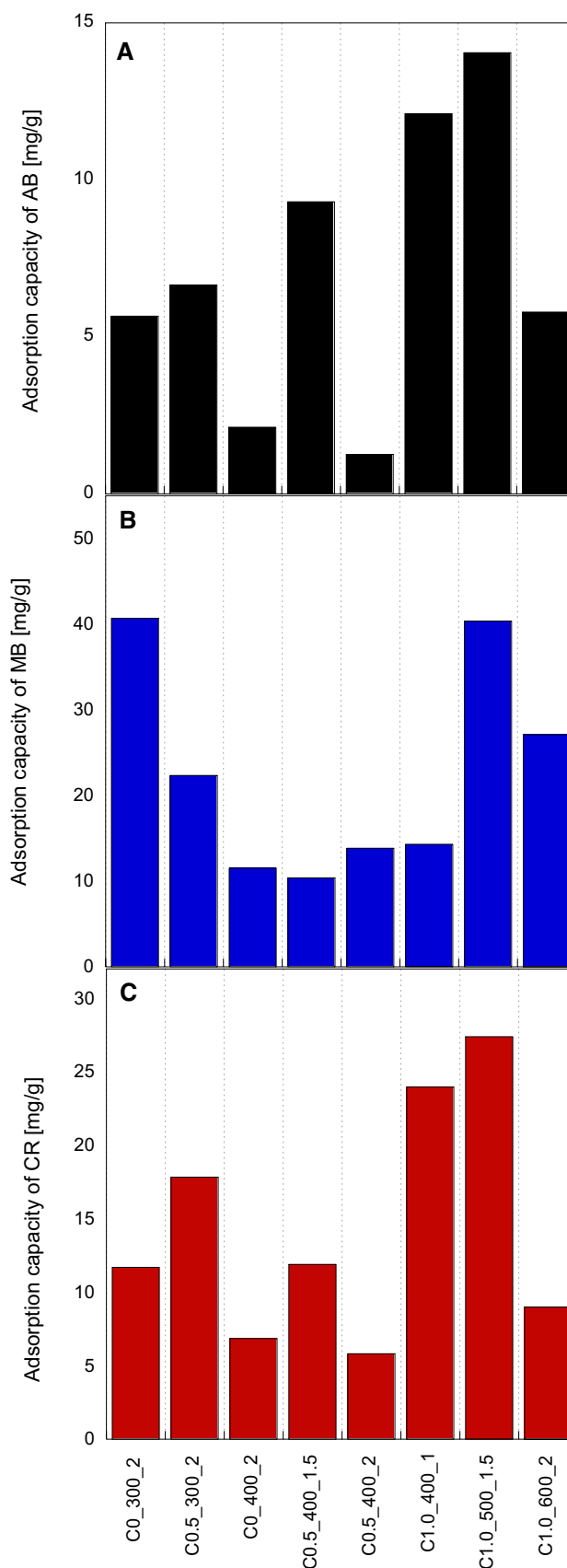
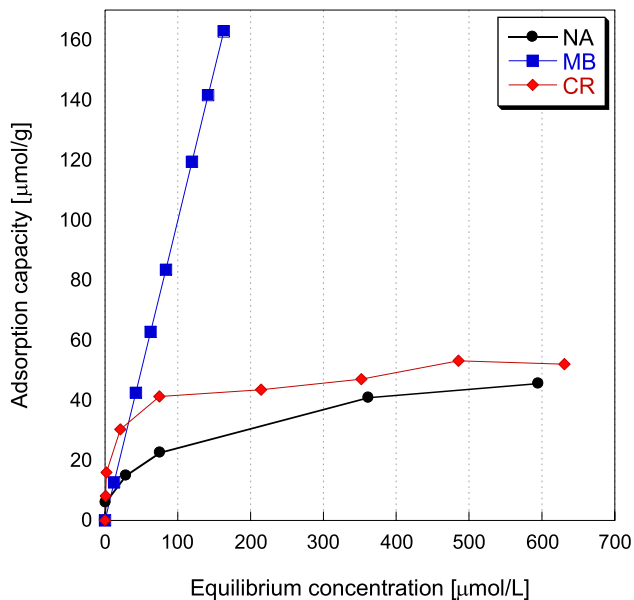


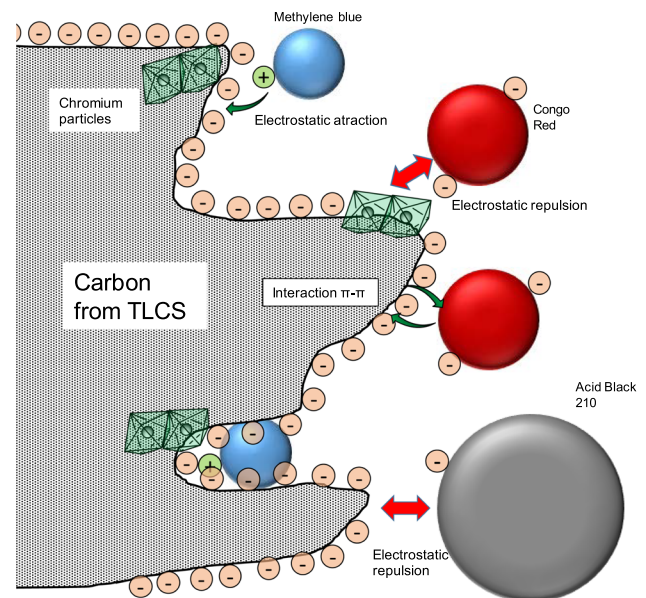
Table 3 Langmuir and Freundlich adsorption isotherms parameters for dyes removal by material C1_500_1.5

Dye	Langmuir			Freundlich		
	Q^{\max} (mmol/g)	b (L/mmol)	R^2	KF (mmol/g) (L/mmol) $^{1/n}$	n	R^2
Methylene Blue	0.1830	2.344	0.9878	0.119	2.411	0.9989
Congo Red	0.0489	122.7	0.9729	0.060	4.902	0.9777
Acid Black 210	0.0510	12.01	0.9935	0.056	2.861	0.9972

**Fig. 7** Adsorption isotherm of the three studied dyes on the material C1_500_1.5 at pH 7 and 25 °C

(Wu et al. 2016), and 3.29 nm for AB (Piccin et al. 2017). It is obvious that AB presents the greatest steric hindrance, for even when adsorbed by means of π - π interactions or an interaction with NH^+ , it exceeds the pore size and therefore its adsorption capacity is limited to that occurring only on the external surface. If one considers the monolayer coverage values from the Langmuir equation (Q^{\max}) and the surface area of this carbon material, MB has a better coverage of 0.091 mmol/g, whereas both CR and AB have a coverage of about 0.025 mmol/g. One can relate the latter to the coverage in the external surface while the former includes the coverage of adsorbed molecules inside the pore system.

Additionally, the team suspected that chromium oxides must be contributing to adsorption by means of electrostatic interaction and surface complexation. Figure 8 represents the proposed adsorption routes for the different dyes employed. It is possible that this material might be subject to regeneration after a thermal treatment or pyrolysis (Corda and Kini 2018).

**Fig. 8** Schematization of the main interactions of dyes with the surface of the carbon materials, illustrating how methylene blue adsorption is driven by electrostatic attraction, whereas Congo red and acid black 210 can only be adsorbed by means of π - π interactions, the later not being able to penetrate in the pore system

Conclusions

The present work demonstrated that it is possible to obtain carbon materials by using CTLS. The various conditions employed during synthesis were found to have a significant effect upon the properties of the materials, mainly on their surface chemistry and structure. Sufficient surface area for adsorption was only developed when high temperatures and a chemical activating agent (ZnCl_2) were employed. Additionally, chromium content was maintained below 1% in the materials, and no evidence of the formation of Cr(VI) was observed. Acidic materials have a negatively charged surface at the adsorption pH and favor the adsorption of small protonated molecules (like methylene blue). On the other hand, bulky molecules, such as Congo Red and Acid Black 210, are adsorbed mainly by

π - π interactions. The present work demonstrated how the synthesis conditions are relevant for developing valorized materials capable of removing various dyes from aqueous solution. The present results postulate that it is possible to valorize wastes from the tannery industry into useful dye adsorbents. In our following work the team will study the extraction of chromium from the CTLS prior to carbon production.

Supplementary Information The online version contains supplementary material available at <https://doi.org/10.1007/s13201-022-01734-z>.

Acknowledgements The technical assistance of Catalina de la Rosa Juarez and Ernesto Ornelas from CIATEC is appreciated. The authors recognize support from LINAN and LANBAMA National laboratories at IPICYT, as well as from Ana Iris Maldonado and Dr. Elizabeth Isaacs Paez for the microscopy analysis and surface area measurements, respectively. The assistance of Dr. Felipe Caballero from CICATA-Altamira in the XRD acquisition is appreciated. Authors appreciate the help of Dr. Richard Lindeke and Dr. Lilja Nielsen in the English language.

Funding This work was funded by the Council for Innovation and Education of the State of Guanajuato (SICES) Grant (262/2019).

Availability of data and material Data will be supplied upon request.

Declarations

Conflict of interest There are no known conflicts of interest associated with this publication and there has been no significant financial support for this work that could have influenced its outcome.

Ethics approval Ethics approval was not required for this study.

Consent to participate Not applicable.

Consent for publication All authors provided consent for publication.

Open Access This article is licensed under a Creative Commons Attribution 4.0 International License, which permits use, sharing, adaptation, distribution and reproduction in any medium or format, as long as you give appropriate credit to the original author(s) and the source, provide a link to the Creative Commons licence, and indicate if changes were made. The images or other third party material in this article are included in the article's Creative Commons licence, unless indicated otherwise in a credit line to the material. If material is not included in the article's Creative Commons licence and your intended use is not permitted by statutory regulation or exceeds the permitted use, you will need to obtain permission directly from the copyright holder. To view a copy of this licence, visit <http://creativecommons.org/licenses/by/4.0/>.

References

Ahmad A, Mohd-Setapar SH, Chuong CS, Khatoun A, Wani WA, Kumar R, Rafatullah M (2015) Recent advances in new generation dye removal technologies: novel search for approaches to reprocess wastewater. RSC Adv. <https://doi.org/10.1039/C4RA16959J>

- Arcibar-Orozco JA, Barajas-Elias BS, Caballero-Briones F, Nielsen L, Rangel-Mendez JR (2019) Hybrid carbon nanochromium composites prepared from chrome-tanned leather shavings for dye adsorption. Water Air Soil Pollut. <https://doi.org/10.1007/s11270-019-4194-x>.
- Bandosz TJ, Jagiello J, Contescu C, Schwarz JA (1993) Characterization of the surfaces of activated carbons in terms of their acidity constant distributions. Carbon. [https://doi.org/10.1016/0008-6223\(93\)90072-1](https://doi.org/10.1016/0008-6223(93)90072-1)
- Chen H, Wang X, Li J, Wang X (2015) Cotton derived carbonaceous aerogels for the efficient removal of organic pollutants and heavy metal ions. J Mater Chem A. <https://doi.org/10.1039/C5TA02999K>
- Corda NC, Kini MS (2018) A review on adsorption of cationic dyes using activated carbon, MATEC Web of Conferences, EDP Sciences, 2018, p. 02022.
- Elaziouti A, Ahmed B (2011) ZnO-assisted photocatalytic degradation of congo Red and benzopurpurine 4B in aqueous solution. J Chem Eng Process Technol. <https://doi.org/10.4172/2157-7048.1000106>
- Erdem M (2006) Chromium recovery from chrome shaving generated in tanning process. J Hazard Mater. <https://doi.org/10.1016/j.jhazmat.2005.08.021>
- Foo KY, Hameed BH (2010) Insights into the modeling of adsorption isotherm systems. Chem Eng J. <https://doi.org/10.1016/j.cej.2009.09.013>
- González GC, Alonso AA, Torre-Marín GC (2017) Innovación tecnológica y curtiduría en el estado de Guanajuato. Economía Informa. <https://doi.org/10.1016/j.ecin.2017.01.005>
- Kannan N, Sundaram MM (2001) Kinetics and mechanism of removal of methylene blue by adsorption on various carbons—a comparative study. Dyes Pigm. [https://doi.org/10.1016/S0143-7208\(01\)00056-0](https://doi.org/10.1016/S0143-7208(01)00056-0)
- Kantarli IC, Yanik J (2010) Activated carbon from leather shaving wastes and its application in removal of toxic materials. J Hazard Mater. <https://doi.org/10.1016/j.jhazmat.2010.03.012>
- Louarrat M, Rahman AN, Bacaoui B, Yaacoubi Y (2017) Removal of chromium Cr (VI) of tanning effluent with activated carbon from tannery solid wastes. Am J Phys Chem. <https://doi.org/10.11648/j.ajpc.20170606.11>.
- Marsh H, Reinoso FR (2006) Activated carbon.
- Nieto-Delgado C, Terrones M, Rangel-Mendez JR (2011) Development of highly microporous activated carbon from the alcoholic beverage industry organic by-products. Biomass Bioenergy. <https://doi.org/10.1016/j.biombioe.2010.08.025>
- Olafsson PG, Bryan AM (1970) Evaluation of thermal decomposition temperatures of amino acids by differential enthalpic analysis. Microchim Acta. <https://doi.org/10.1007/BF01225712>
- Oliveira LC, Coura CVZ, Guimarães IR, Gonçalves M (2011) Removal of organic dyes using Cr-containing activated carbon prepared from leather waste. J Hazard Mater. <https://doi.org/10.1016/j.jhazmat.2011.06.014>
- O'Neil MJ (2013) The Merck index—an encyclopedia of chemicals, drugs, and biologicals, Cambridge, UK.
- Pati A, Chaudhary R, Subramani S (2014) A review on management of chrome-tanned leather shavings: a holistic paradigm to combat the environmental issues. Environ Sci Pollut R. <https://doi.org/10.1007/s11356-014-3055-9>
- Piccin JS, Guterres M, Salau NPG, Dotto GL (2017) Mass transfer models for the adsorption of Acid Red 357 and Acid Black 210 by tannery solid wastes. Adsorpt Sci Technol. <https://doi.org/10.1177/0263617416675624>
- Silverstein RM, Webster FX, Kiemle DJ (2005) Spectrometric identification of organic compounds.
- Sposito G (1998) On points of zero charge. Environ Sci Technol. <https://doi.org/10.1021/es9802347>

- Sundar VJ, Raghavarao J, Muralidharan C, Mandal AB (2011) Recovery and utilization of chromium-tanned proteinous wastes of leather making: a review. *Crit Rev Environ Sci Technol*. <https://doi.org/10.1080/10643389.2010.497434>
- Tan KB, Vakili M, Horri BA, Poh PE, Abdullah AZ, Salamatinia B (2015) Adsorption of dyes by nanomaterials: recent developments and adsorption mechanisms. *Sep Purif Technol*. <https://doi.org/10.1016/j.seppur.2015.07.009>
- Weiss IM, Muth C, Drumm R, Kirchner HOK (2018) Thermal decomposition of the amino acids glycine, cysteine, aspartic acid, asparagine, glutamic acid, glutamine, arginine and histidine. *BMC Biophys*. <https://doi.org/10.1186/s13628-018-0042-4>
- Wu Q-Y, Liang H-Q, Li M, Liu B-T, Xu Z-K (2016) Hierarchically porous carbon membranes derived from PAN and their selective adsorption of organic dyes. *Chin J Polym Sci*. <https://doi.org/10.1007/s10118-016-1723-6>

Publisher's Note Springer Nature remains neutral with regard to jurisdictional claims in published maps and institutional affiliations.